HHS Public Access

Author manuscript

*Biomaterials*. Author manuscript; available in PMC 2018 September 01.

Published in final edited form as:

*Biomaterials*. 2017 September ; 138: 35–45. doi:10.1016/j.biomaterials.2017.05.034.

# Revisiting the Value of Competition Assays in Folate Receptor-Mediated Drug Delivery

**Steven K. Jones**[a], **Anwesha Sarkar**[c], **Daniel P. Feldmann**[a], **Peter Hoffmann**[c], and **Olivia Merkel**[a,b,d,e,*]

[a]Department of Oncology, Wayne State University School of Medicine, Detroit, MI

[b]Department of Pharmaceutical Sciences, Wayne State University School of Pharmacy and Health Sciences, Detroit, MI

[c]Department of Physics and Astronomy, Wayne State University of College of Liberal Arts and Sciences, Detroit, MI

[d]Department of Pharmacy, Pharmaceutical Technology and Biopharmacy, Ludwig-Maximilians-Universität München, Munich, Germany

[e]Nanosystems Initiative Munich (NIM), Ludwig-Maximilians-Universität München, Munich, Germany

## Abstract

Polymeric nanoparticles have been studied for gene and drug delivery. These nanoparticles can be modified to utilize a targeted delivery approach to selectively deliver their payload to specific cells, while avoiding unwanted delivery to healthy cells. One commonly over-expressed receptor which can be targeted by ligand-conjugated nanoparticles is the folate receptor alpha (FRα). The ability to target FRα remains a promising concept, and therefore, understanding the binding dynamics of the receptor with the ligand of the nanoparticle therapeutic can provide valuable insight. This manuscript focuses on the interaction between self-assembled nanoparticles decorated with a folic acid (FA) ligand and FRα. The nanoparticles consist of micelles formed with a FA conjugated triblock copolymer (PEI-g-PCL-b-PEG-FA) which condensed siRNA to form micelleplexes. By combining biological and biophysical approaches, this manuscript explores the binding kinetics and force of the targeted siRNA containing nanoparticles to FRα in comparison with free FA. We demonstrate via flow cytometry and atomic force microscopy that multivalent micelleplexes bind to FRα with a higher binding probability and binding force than monovalent FA. Furthermore, we revisited why competitive inhibition studies of binding of multivalent nanoparticles to their respective receptor are often reported in literature to be inconclusive evidence of effective receptor targeting. In conclusion, the results presented in this paper suggest that multivalent targeted nanoparticles display strong receptor binding that a

*Corresponding author: Prof. Dr. Olivia Merkel, Department of Pharmacy, LMU München; Butenandtstr. 5-13 (Haus B), D 81377 München, Germany; Tel. 089 2180 77025, FAX 089 2180 77020, Olivia.merkel@LMU.de.

monovalent ligand may not be able to compete with under *in vitro* conditions and that high concentrations of competing monovalent ligands can lead to measurement artifacts.

## Graphical abstract

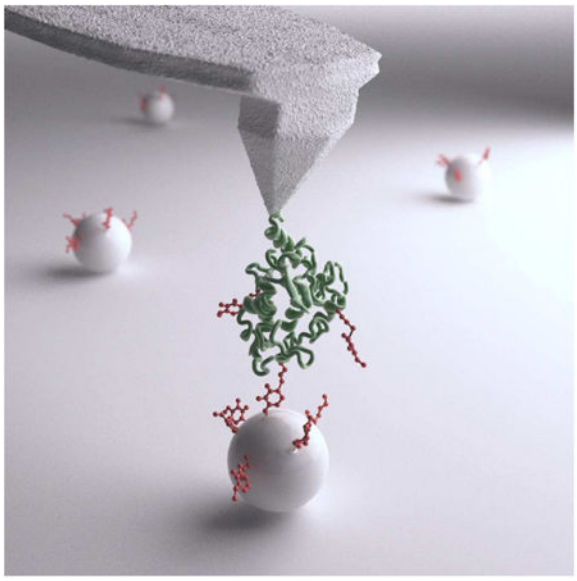

### Keywords

Folate Receptor Targeting; siRNA delivery; Polymer Micelleplexes; Atomic Force Microscopy; Competitive Uptake; Receptor Ligand Interaction; Affinity

## Introduction

Smart personalized cancer therapies utilize the molecular profiles of the tumor of individual patients as the basis of treatment and can selectively target malignant cells over healthy ones. A promising approach, which has already been utilized by drugs approved by the FDA, is based on targeting cellular receptors which are over-expressed on the malignant cells. Several studies have been described which utilize receptor targeting to deliver a wide variety of payloads to multiple disease states.(1, 2) Several cancers such as ovarian, non-small cell lung cancer, kidney, and colorectal have a significant over-expression of folate receptor alpha (FRα). In ovarian cancer patients, it has been noted that as the histological grade of the cancer increases, so do the FRα expression levels. FRα over-expression in malignant cells along with their very low expression throughout the rest of the body, makes for a promising receptor for targeted drug delivery.(3-5) FRα internalization can be exploited by hijacking the cells' natural internalization process with a drug payload which is conjugated to the folic acid.(6, 7) Currently, several approaches to FRα guided imaging and therapies are being utilized clinically and tested in clinical studies.

However, to improve and better understand FRα drug targeting, the mechanics behind the ligand-receptor interaction need to be better understood. With a variety of targeting

strategies for FRα, the need to comprehend the advantages and disadvantages to designing a FRα targeted approach is necessary and will lead to more successful therapeutic approaches. One key aspect that has been studied is the need for having a monovalent versus multivalent drug conjugate. Several studies, including the clinical studies performed by Endocyte have proven that monovalent studies can be successful and deliver their drug payload specifically to cells which over-express FRα, while decreasing any unwanted and off target side effects. (8-11) Conversely, many studies, such as the ones by Silpe et. al. and Stella et. al., have demonstrated that a multivalent approach yields a more advantageous system.(12, 13) In the latter studies, the principle idea of adding multiple folic acid molecules on the surface of the drug carrier is aimed at promoting higher binding avidity and affinity to FRα than a monovalent folic acid delivery system. This idea relies on the fact that several FRα cluster on the cell surface within lipid rafts, and therefore, multiple ligands binding to multiple receptors increase and prolong ligand-receptor interactions and therefore increase the FRα internalization with the drug.(12, 14, 15) Studies performed by Silpe et. al. and Leistra et. al. revealed that with multiple ligand binding domains, the binding strength to the receptor of the folic acid drug conjugates can increase up to several orders of magnitude and 1,000-fold, respectively.(12, 14) Conversely, it has been shown that multivalent agents, such as the nanobodies used by Movahedi et. al., bind more strongly to off-target tissues.(16) There are abundant nanocarrier delivery systems that have been used for FR-targeted delivery of a payload, such as siRNA. Of these systems, previous studies with block copolymers consisting of polyethylene imine (PEI), polycaprolactone (PCL), and poly ethylene glycol (PEG), or PEI-PCL-PEG, have demonstrated effective siRNA delivery through effectively shielding and condensing siRNA in so-called micelleplexes at suitable sizes and zeta potentials for substantial protein knockdown.(17-20) Additionally, when this PEI-PCL-PEG platform was further modified with a folic acid targeting moiety, the self-assembling nanoparticles can selectively target and deliver siRNA to cancer cells which over-express FRα. (21, 22)

This manuscript focuses on understanding the interaction of these multivalent FRα targeted nanoparticles with the receptor in more detail. To advance nanoparticle and small molecule therapies which utilize receptor mediated drug delivery, a thorough understanding of the receptor-ligand interaction is imperative. Here, we assess this interaction with multiple *in vitro* cell based and biophysical techniques. Collectively, we demonstrate that excess monovalent free folic acid cannot outcompete targeted multivalent micelleplexes for the binding to the clustered FRα and that by adding multiple ligands to the surface of the nanoparticle, a higher binding avidity is achieved. Additionally, the presence of high concentrations of competing ligand can cause instability problems or aggregation of the delivery system. These effects must be taken into consideration while validating targeted delivery with nanoparticles. Here, we demonstrate that pretreatment with excess ligand may not be the best approach in determining the specificity of targeting effects and alternative approaches are offered.

## Materials and Methods

### Materials

PEI-PCL-PEG and PEI-PCL-PEG-FA copolymers were synthesized as described before.(22) Briefly, ring opening polymerization of polycaprolactone (PCL) and hetero-bifunctional (HO-PEG-COOH, 3.5 and 5 kDa) PEG was performed for the targeted polymer. For non-targeted PEI-PCL-PEG, monofunctional (CH3-PEG-COOH, 5 kDa) PEG (JenKem Technologies, United States) was used instead. Acrylate-PCL-*b*-PEG-alkyne or acrylate-PCL-*b*-mPEG was reacted with hyper branched polyethylenimine (hyPEI, 25k Da, BASF, Ludwigshafen, Germany) in a Michael addition, and azido functionalized folic acid was coupled to the alkyne-modified PEG in a click reaction. Firefly luciferase (FLuc) dicer substrate double-stranded siRNA (sense: 5′-pGGUUCCUGGAACAAUUGCUUUUAca-3′, antisense: 3′-GACCAAGGACCUUGUUAACGAAAAUGU-5′, where p denotes a phosphate residue, lower case bold letters are 2′-deoxyribonucleotides, capital letters are ribonucleotides and underlined capital letters are 2′-O-methylribonucleotides) (DsiRNA), and Alexa Fluor-488 labeled siRNA was purchased from Integrated DNA Technologies (IDT, Coralville, IA).

### Preparation of PEI-g-PCL-b-PEG-Fol micelleplexes for *in vitro* use

Each polymer was dissolved in sterile water to yield a 1 mg/mL concentration of the PEI block of the polymer. Once dissolved, samples were filtered through a 0.22 μm filter for sterilization. In order to prepare the micelleplexes, a specific ratio between the amine groups found within the polymer (N) and the phosphate groups of the siRNA (P) was chosen, as described before. (22)

To prepare the micelleplexes, equal volumes of diluted polymer and siRNA were pipetted together, vortexed quickly, and let incubate at room temperature for 20 minutes. After 20 minutes, the freshly formed polyplexes were characterized or used in cell culture experiments.

### Hydrodynamic Diameter and Zeta (ζ) Potential Measurements

Measurements of the hydrodynamic diameters of micelleplexes were performed by dynamic light scattering (DLS) using a Zetasizer Nano ZS (Malvern Instruments Inc., Malvern, UK) as described previously. (22) Micelleplexes were made as described above in 1× PBS and measured at N/P 5 complexing with 40 pmol of siRNA. Samples were diluted with 1× PBS solution to a total volume of 75 μL within a disposable cuvette. Each sample was read in triplicates with each run consisting of 15 scans. Results are represented as average size (nm) ± standard deviation. The samples were then diluted with 1× PBS to a final volume of 800 μL, and transferred to a disposable capillary cell where ζ-potential measurements were performed. ζ-potential measurements were read in triplicates by laser Doppler anemometry (LDA), with each run consisting of 30 scans. Results are shown in average mV ± standard deviation.

## Cell Culture

SKOV-3 and IGROV-1 cell lines are human ovarian cancer cell lines which were obtained from ATTC (LG Promochem, Wesel, Germany). Additionally, SKOV-3/LUC cells stably expressed the reporter gene luciferase were established as described before.(23) All three ovarian cancer cell lines were cultured in folate free DMEM cell culture medium (Sigma-Aldrich) supplemented with L-glutamine, sodium bicarbonate, 10% fetal bovine serum (Thermo Scientific Hyclone), and 1% penicillin/streptomycin. Cells were allowed to grow at 37 °C and 5% $CO_2$ and were passaged every 2-3 days when they had reached confluency.

## Folate Receptor Alpha Receptor Expression Profiles by Flow Cytometry

Human ovarian cancer SKOV-3 and IGROV cells were grown in folate free DMEM medium and subcultured as described previously.(22) For receptor expression experiments, 200,000 cells were harvested per tube and centrifuged at 350 g for 5 min. After the cells were pelleted, the supernatant was decanted, and the cells were washed twice with 1× PBS + 2 mM EDTA. Following an additional centrifugation step, 20 μL of primary monoclonal mouse anti-human Folate Receptor α antibody (MOV18 Enzo Life Sciences, Farmingdale, NY, USA) was added to their appropriate tubes. Samples were vortexed and incubated for 25 minutes at 4° C in the dark. Cells were washed with 1× PBS + 2 mM EDTA, centrifuged and washed one more time. The supernatant was decanted and 20 μL of a secondary goat anti-mouse IgG pacific blue conjugate antibody (Invitrogen, Carlsbad, CA, USA) was added to the tubes. After addition, samples were vortexed and incubated for 25 minutes at 4° C in the dark. Following this incubation step, samples were washed with 1× PBS + 2 mM EDTA twice. Samples were analyzed via flow cytometry (Applied Biosystems Attune Acoustic Focusing Cytometer), and the Median Fluorescence Intensity (MFI) was recorded. Samples were run in triplicates, with each sample consisting of a minimum of 10,000 viable cells. The secondary antibody was excited at 410 nm, and emission detected using a 450/40 band-pass filter set. Analysis and presentation of the data was performed in the GraphPad Prism 5.0 software calculating mean values and standard deviation.

## Cellular Uptake of Micelleplexes by Flow Cytometry

In a 24-well plate (Corning Incorporated, Corning, NY) 60,000 SKOV-3 cells were seeded and incubated overnight at 37 °C and 5% $CO_2$. In order to remove any folic acid in the well, cells were washed two times with ice cold acid wash solution (150 mM NaCl, 10 mM sodium acetate, pH 3.5), followed by three washes with ice cold HBSS buffer (pH 7.4). Afterwards, serum free and folate free DMEM media (Sigma-Aldrich, St. Louis, MO, USA) was added to each well for samples treated in the absence of folic acid to avoid any source of folic acid. Samples that were treated with excess free folic acid (in varying concentrations) were treated with serum free DMEM media containing the specific quantity of folic acid. Samples were incubated in the new media for 30 minutes before transfection. For transfection, 50 μL of freshly made micelleplexes containing 50 pmol of AF488 siRNA at varying N/P ratios were added per well. Negative controls consisted of blank/untreated cells while positive control cells were transfected with Lipofectamine 2000 (Life Technologies, Carlsbad, CA, USA) following the supplier's standard transfection protocol. Unless otherwise stated, cells were transfected for 4 hours in 37 °C and 5% $CO_2$ with 50 μL

of micelleplex solution containing 50 pmol siRNA within a total volume of 500 μL of serum free and folate free DMEM media (Sigma-Aldrich, St. Louis, MO, USA). After incubation, media was removed, and 100 μL of 0.4% Trypan Blue (Fisher Scientific, Waltham, MA, USA) was added to each well in order to quench any extracellular fluorescence. Cells were then washed twice with 1× PBS + 2 mM EDTA, trypsinized and spun down at 350 g for 5 min. After centrifugation, the supernatant was decanted, and the cells were washed twice with 1× PBS + 2 mM EDTA. Samples were analyzed via flow cytometry, and the Median Fluorescence Intensity (MFI) was recorded. Samples were run in triplicates, with each sample consisting of a minimum of 10,000 viable cells. The siRNA was excited at 488 nm, and emission detected using a 530/30 band-pass filter set. Analysis and presentation of the data was performed in GraphPad Prism 5.0 software calculating mean values and standard deviation.

## Protein Knockdown by Luciferase Assay

Protein knockdown was measured with luciferase knockdown experiments. SKOV-3/LUC cells stably transfected with a luciferase encoding plasmid (1649 bp), pTRE2hyg-LUC (Clontech, Sait-Germain-en-Lye, France) that contains a CMV promoter.(24) In 24 well plates, 60,000 SKOV-3/LUC cells were seeded per well and incubated overnight at 37 °C and 5% $CO_2$. To remove any folic acid in the well, cells were washed two times with ice cold acid wash solution as described above, followed by three washes with ice cold HBSS buffer. Afterwards, serum free and folate free DMEM media was added to each well for samples treated in the absence of folic acid. Samples that were tested in the presence of excess free folic acid were treated with serum free DMEM media containing the specific quantity of folic acid in order to match the concentrations used in the uptake studies. Samples were incubated in the new media for 30 minutes before transfection. Micelleplexes were made as described previously with 50 pmol of luciferase targeted siRNA. Cells were incubated at 37 °C and 5% $CO_2$. After 48 hours, cells were washed twice with 200 μL of PBS and treated with 300 μL of lysis buffer (Cell Culture Lysis Reagent, CCLR, Promega, Madison, WI, USA) per well. Each well was scraped with a pipette to effectively dislodge cell debris on the bottom of the well. The plate was then rocked for 5 minutes at room temperature. Cell lysates were transferred to conical tubes and set on ice. Each tube was vortexed for 10-15 seconds and then centrifuged at 12,000 g for 2 minutes at 4 °C. The supernatant was collected, and 20 μL of each sample was added to a white 96-well plate to be analyzed for luminescence using a Synergy 2 microplate reader (BioTek Instruments, Winooski, VT, USA). Each well was injected with 100 μL of luciferase assay reagent containing 10 mM luciferin (Sigma-Aldrich, St. Louis, MO, USA) by the plate reader immediately before the measurement. Samples were measured in triplicates and analyzed using GraphPad Prism 5.0 software representing average values and standard deviation.

## Monensin Assay

To determine the extent of siRNA being trapped within the endosome, a monensin assay was utilized and analyzed via flow cytometry. In 24-well plates, 60,000 SKOV-3 cells were seeded and incubated overnight at 37 °C and 5% $CO_2$. Freshly made micelleplexes containing 50 pmol of AF488 siRNA were added per well. Negative controls consisted of blank/untreated cells. Cells were transfected for 24 hours in 37 °C and 5% $CO_2$ with 50 μL

of micelleplex solution containing 50 pmol siRNA within a total volume of 500 μL of serum containing cell culture media. In order to quench any extracellular fluorescence, triplicates of cells were incubated with 100 μL of 0.4% Trypan Blue while other triplicates were treated with 50 μM monensin. Cells were then washed twice with 1× PBS + 2 mM EDTA, trypsinized and spun down at 350 g for 5 min. After centrifugation, the supernatant was decanted, and the cells were washed once with 1× PBS + 2 mM EDTA and incubated at 4 °C for 30 minutes with 50 μM monensin. Afterwards, cells were washed once with 1× PBS + 2 mM EDTA and were analyzed via flow cytometry; the Median Fluorescence Intensity (MFI) was recorded for each sample. Samples were run in triplicates, with each sample consisting of a minimum of 10,000 viable cells. The siRNA was excited at 488 nm, and emission detected using a 530/30 band-pass filter set. Analysis and presentation of the data was performed in the GraphPad Prism 5.0 software calculating mean values and standard deviation. Results were compared between cells treated with and without Trypan Blue and monensin in order to gain insight on the targeted and non-targeted micelleplex uptake profile.

### Atomic Force Microscopy (AFM)

Atomic Force Microscopy was used in order to assess the size and morphology of the micelleplexes after siRNA condensation. Additionally, binding events of folate decorated polyplexes compared to folic acid on a folate receptor modified cantilever were measured as described below. For AFM size and morphology measurements, micelleplexes were prepared at N/P 5 with 40 pmol of non-fluorescent siRNA in a total volume of 20 μL in 5% glucose. That suspension was added to a glass coverslip and let dry overnight. Lastly, micelleplexes for AFM force measurements with a FRα modified cantilever were prepared as described above with 75-fold higher amounts of siRNA and polymer in order to obtain a 3 mL suspension with the same polymer and siRNA concentration in 5% glucose solution as used for all other AFM experiments.

### Modification of Cantilevers with Folate Receptor

Cantilevers (MLCT-Bio, Bruker) were incubated within a cleaning solution (Cell cleaning solvent for UV/VIS, Agilent Technologies) for 2 h. The cantilevers were cleaned with ultra DI water afterwards. Organic contaminants were removed through ozone treatment for 20 min. Afterwards, 5 mL of a 1 mM solution of silane PEG NHS (3400 Da, ThermoScientific) in 95% Ethanol and 5% DI water was prepared, and the cantilever was incubated in this solution for 2 h. After rinsing, the cantilever was incubated in a solution of 0.15 mL recombinant human folate receptor α (FOLR1) protein (EZ Biosystems, College Park, MD, USA) for 1 h. Afterwards, the cantilever was preserved in 1×PBS solution until the experiments were performed within the following 24 h.

### Immobilization of Folic Acid or Folate Decorated Particles on the Substrate

Small silicon square pieces (15×15 mm) were rinsed with ultra DI water and UV glued to the bottom of a 60 mm sterile petri dish. The petri dish and substrate were further cleaned with DI water. The silicon substrate was incubated in a 5 mL solution of 1 mM silane PEG NHS (3400 Da, Thermo Scientific) in 95% Ethanol and 5% DI water for 2 h, followed by incubation in either 5 mL DMSO solution of 5 mg/mL folic acid (2.25 mM) or a suspension

of folate decorated particles (16.38 μM of folic acid) for 5 h. The substrate was then washed with DI water and preserved in 1× PBS buffer until the experiment was performed.

## Results and Discussion

The strategic design of the targeting aspect of the triblock copolymers used here for siRNA delivery relies upon the inherent over-expression of FRα in a variety of cancers. The American Cancer Society (ACS) estimates that over 85% of ovarian cancers significantly over-express FRα, and that the expression has a positive correlation with the histological grade of the cancer. (4) Therefore, FRα levels have been studied in ovarian cancer cell lines such as IGROV-1 and SKOV-3 also by others. Both cell lines show significantly upregulated FRα expression levels when compared to normal epithelial tissues and other cancerous cell lines such as A549 adenocarcinoma alveolar basal epithelial cells. (25, 26). Figure 1 represents FRα expression levels in the specific cell lines used here and clearly demonstrates that both ovarian cancer cell lines IGROV1 and SKOV-3 showed an increase in FRα status. It should be noted that with varying FRα expression profiles, the receptor recycling rate does not change. Therefore, SKOV-3 cells were utilized in all *in vitro* experiments to be consistent with previously published results.(21, 22)

For nanoparticles to successfully deliver their payloads, two important characteristics that need to be considered are their hydrodynamic diameter and zeta potential. The polymers used here for nanoparticle formation were previously characterized by $^{1}$H NMR, UV spectroscopy, and absorbance measurements. (22) The polymers used in this study were selected for the following reasons: 1) the FRα targeted polymer has previously demonstrated efficient cytosolic delivery of siRNA,(22) and 2) the polymer termed “mixed conjugate” contains the highest folic acid weight percentage on the surface of the micelleplexes, and 3) the null folate conjugate does not contain any folic acid and therefore can be used as a negative control. Due to the conditions needed to carry out the AFM force measurements, the hydrodynamic diameter and zeta potentials were determined in PBS buffer. As shown in Figure 2A, in all cases, hydrodynamic diameters were slightly larger than observed in 5% glucose solution (22) but still at or below the 260 nm threshold reported in literature to favor evasion of recognition by macrophages. (27-29) It was not surprising that the hydrodynamic diameter increased when changing the buffer from 5% glucose to a buffer with higher ionic strength where the hydrodynamic diameter is determined in the presence of a larger amount of counter ions that move with the diffusing particles. The sizes of the micelleplexes are comparable with other folate receptor targeted nanoparticles. Bhattacharya, Li, and Esmaeili et. al. all have successfully synthesized nanoparticles around 100-200 nm in size, while others such as Krais and Su et. al. reported sizes greater than 300 nm. (30-34) Interestingly, the polydispersity indices (PDIs) were smaller than observed in glucose solution with 0.11, 0.12, and 0.04 for targeted, mixed conjugate, and null folate micelleplexes, respectively. The low PDI for each micelleplex shows that size distribution around the average hydrodynamic diameter is very narrow, and no large aggregates were observed. The same suspensions were then taken and utilized for zeta potential measurements. The micelleplexes made with all three conjugates had a slightly positive charge, between +1.5 and +3 mV as shown in Figure 2B. This positive charge can support the initial interaction between the negatively charged cellular membrane and the positive charge of the outer shell of the polyplex but should not

over shadow the desired targeting effect of the folic acid ligand. Taken together, in PBS, the three chosen conjugate formulations had hydrodynamic diameters and zeta potentials that were comparable to previous findings, which demonstrates initial promise towards an effective nanoparticle siRNA delivery approach based on size and zeta potential criteria.

When assessing receptor targeting, a common way to assess specificity and receptor mediated endocytosis is to inhibit the uptake with an excess of the free endogenous ligand of the receptor. (22, 35-39) Accordingly, in regards to folate receptor targeting, free folic acid has been used as the substrate to demonstrate competitive inhibition for the binding and internalization for folate decorated therapies. Within recent literature, concentrations of excess folic acid used to inhibit nanoparticle binding and uptake have ranged from as low as 100 μM up to 5 mM. However, due to folic acid being a small molecule with only one possible binding interaction with the receptor, and the nanoparticles used within this manuscript being multivalent, we wanted to better understand the potential inhibition of nanoparticle binding to the folate receptor that free folic acid can mediate. Therefore, we used a concentration range of free folic acid that covers the concentrations reported in the literature. As shown in Figure 3, we compared micelleplexes made with the targeted polymer against null folate micelleplexes with and without excess competing free folic acid. Hypothetically, the folic acid decorated micelleplexes would experience an inhibition in their uptake via FRα in the presence of an excess folic acid, while the null folate conjugates uptake profiles would not be affected. However, due to the multivalent nature of the conjugates, we did not expect strong inhibition of their binding or uptake due to their stronger binding avidity to FRα compared to folic acid. As described in our previous publication, as well as in Figure 3 A, only a slight inhibition of uptake of the targeted nanoparticles is observed, while the uptake of the null folate micelleplexes is unaffected at low excess FA concentrations. (22) This slight inhibition at low concentrations is in corroboration with what the Stayton group has demonstrated. (35) However, as the concentration of the free folic acid increased to 500 μM and above (Figure 3 B-D), not only was the targeted nanoparticle uptake diminished, but also that of the null folate nanoparticles. It should be noted that uptake was studied 4 h post transfection. After such a short incubation time, the targeting advantage of the targeted micelleplex over the null folate one is not expected. This assumption is based on previously published results demonstrating that targeted micelleplexes do not achieve a significant enhancement of siRNA delivery until time points exceeding 4 hours as well as the recycling rate of FRα being 5.7 hours.(22, 40) Collectively, the data in Figure 3 illustrates that at low concentrations of folic acid, a minor inhibition of the targeted conjugate occurred, while not affecting the null folate conjugate which is taken up by routes other than receptor-mediated endocytosis. However, when treated with higher concentrations of free folic acid, it is possible that the hydrophobic FA destabilizes all micelles, no matter if they are targeted or not, which leads to decreased siRNA delivery for all nanoparticles.(41) It is also possible that the DMSO containing solvent in which folic acid is dissolved changes the viscosity of the media, the micelle stability, or affects the cells. This decrease in nanoparticle uptake of targeted and non-targeted formulations after addition of high amounts of FA to the system has been observed before with folate targeted liposomes by Lee et al.(41) In order to overcome the stronger binding affinity observed in case of multivalent particles, excess amounts of folic acid, above

1 mM were required. However, at these high concentrations, inhibition of the uptake of non-targeted liposomes was measured as well, which corroborates the results shown here in Figures 3 B-D. (41, 42) Lee et al. reasoned that with excess folic acid in solution, a disruption of the cationic lipid/nucleic acid complex stability occurred. Also in the case of our micelles, disruption and premature release of siRNA is possible in the presence of excess folic acid but was not observed (data not shown). However, at excess folic acid concentrations as low as 250 μM, hydrodynamic diameters of higher than 600 nm were observed, and steadily continued to increase with the folic acid concentration. These hydrodynamic diameters measured by the DLS clearly suggest that aggregation is occurring in the presence of free folic acid. It should be noted, however, that folic acid has been described to form dimers and trimers at higher concentrations within a system. These dimers and trimers, if formed, are then unable to bind to FRα. (43) Therefore, as shown in literature, higher concentrations of folic acid on the surface of multivalent FA-modified nanoparticle may not necessarily yield a greater targeting advantage but rather hinder the targeting system. Reddy et. al. revealed that only 0.03 molar percent of folic acid on a liposome is needed to gain a targeting advantage. With higher molar percentages of FA on the surface of nanoparticles, it is possible that the problem of FA dimer and trimer formation is encountered. (42) The binding advantage of multivalent particles was demonstrated in uptake studies using SKOV-3 cells *in vitro*. However, when an excess concentration of free folic acid is used to saturate the receptors to outcompete for the binding of the targeted micelleplexes, no competition is detected. This observation falls in line with the hypothesis that multivalent micelleplexes cannot easily be displaced from FRα binding sites by monovalent folic acid. In comparison to the studies performed by Liu et. al., while their polyplexes were shown to be able to be inhibited with low excess amounts of FA added to the system, these micelles demonstrated within this manuscript carry more FA on the surface.(21) This discrepancy can therefore be explained by the difference in valency which determines the affinity and avidity with the receptor and the ability of these multivalent nanoparticles to be displaced by a monovalent ligand or not. Similar observations have been reported not only *in vitro*, but even *in vivo*.(16) However, when high amounts of folic acid are added to the system, the decrease in uptake affects both targeted and non-targeted formulations. This suggests that the inhibition occurring is not due to blocking the receptor binding studies, but perhaps affecting all nanoparticle uptake due to a cellular event or a physical destabilization of the cationic condensation of the nucleic acids, or aggregation of the micelles, as Reddy hypothesized.(42) Further experiments need to be performed to better understand this effect. Therefore, when performing competitive inhibition studies, the concentration of folic acid in the experiment should be considered and optimized for maintained stability of the delivery system. Furthermore, competition assays may not necessarily be the most efficient route of addressing receptor targeting specificities; especially if the delivery system physical chemical properties are affected due to excess ligand within the system.

After assessing the uptake profiles with and without excess free folic acid, the next step was to determine whether or not protein knockdown was affected by the inhibited uptake. We hypothesized that if the uptake is inhibited for the folate receptor targeted micelleplexes, the knockdown of protein should be inhibited as well. By performing this test, we were able to

assess whether the slightly inhibited uptake was reflected in only a slightly inhibited pharmacologic effect or if uptake mechanisms other than receptor-mediated endocytosis would skew the uptake results but would lead to endosomal entrapment of the particles reflected in a large inhibition of gene knockdown. SKOV-3/LUC cells were incubated with and without 250 μM and 1 mM of free folic acid, while being transfected with siRNA against Firefly Luciferase. After 48 hours, the luciferase knockdown was analyzed. In both data sets, the targeted micelleplexes achieved a significantly greater protein knockdown than the non-targeted micelleplexes. The more efficient gene knockdown mediated by the targeted micelleplexes could be due to the recycling parameters of FRα. The majority of FRα, once it binds and internalizes the ligand, will be recycled back to the cell surface. (40) This prevents many micelleplexes from becoming trapped inside the endosome and counteracts the degradation of the siRNA before it can cause protein knockdown. It is also possible that exocytosed particles may be endocytosed again at a later time point. Data shown in Figure 4A demonstrates that when there was little uptake inhibition with 250 μM free folic acid, as shown in Figure 3 A, there was no knockdown inhibition. This demonstrates that over a prolonged time period, although a slight uptake inhibition occurred at 250 μM excess folic acid after 4 hours, the overall multivalent binding approach eventually overcomes whatever slight inhibition occurs early on and therefore negates any offset in knockdown expected. Conversely, Figure 4 B demonstrates that a large excess folic acid (1 mM) can not only inhibit the uptake of both targeted and non-targeted nanoparticles, it can also impede the subsequent knockdown of luciferase no matter if the particles are taken up by receptor-mediated endocytosis or other uptake mechanisms. This data agrees with the uptake results demonstrating that uptake and knockdown seem to be inhibited when high concentrations of folic acid are added to the system due to micelle aggregation or a possible decrease in their stability. It should be noted that due to the relatively slow recycling rate of FRα, most folate receptor ligands remain on the cell surface or recycle through the cell without unloading their cargo into the cytosol.(40) The release from the receptor is expected to occur in the endosome after receptor mediated endocytosis. Therefore, it may take longer for the targeted particles to achieve knockdown, and only a slight improvement of knockdown mediated by targeted versus non-targeted micelleplexes is observed at 48 h post transfection. It should be noted that Moody et al. demonstrated that the recycling rate of transferrin and Her2 receptors was altered and that the cargo was redirected to the lysosome when the receptors were crosslinked with biotinylated cargo and the addition of streptavidin. (44) Therefore, it seems possible that multivalent particles, such as the folate decorated micelleplexes described here, which can bind and occupy multiple receptors on the cell surface, can alter the receptor's natural endocytic pathway to enhance the delivery of therapeutic agents to the lysosome. This agrees with other multivalent FRα targeting studies suggesting that multivalent particles follow a lysosomal pathway to the cytosol. (6, 45)

Theoretically, if the folate decorated micelleplexes bind with FRα and become internalized, the receptor, ligand and nanoparticle will be taken up into the early endosome and undergo the endosomal ripening process starting from early endosomes and eventually merging with lysosomes. However, since the mechanism of action of the RNAi machinery is within the cytosol, our micelleplexes were designed to escape the endosome. A monensin assay is able to delineate where the siRNA loaded micelleplexes are located during a fixed time after

transfection due to the dissipating fluorescent signal though neutralization of endocytic vesicles and prevention of receptor recycling.(46, 47) With trypan blue treatment in addition to monensin, observations can be made as to where specifically the siRNA loaded micelleplexes are localized after transfection. As shown in Figure 5, after 48 hours, the folic acid decorated particles (targeted) display significantly higher association with SKOV-3 cells than the null folate particles. However, much of the siRNA seems to be present extracellularly and intravesicularly. The small difference of cytosolic siRNA after delivery with the targeted versus non-targeted micelleplexes at the 48 h time point clearly explains the small benefit of targeting on gene knockdown efficacy at the same time point. These data could be explained by the relatively slow recycling kinetic of FRα. As a result of most FRα being recycled back to the cell surface with the folic acid still attached delivery difficulties for FRα mediated targeting strategies have been reported due to drugs not being able to escape the endosome after their first internalization do not reach the cytosol of the cell on first pass into the cell. The recycling of the targeted nanoparticles back to the cell surface, combined with the slow internalization kinetics of FRα, could explain the increased extracellular and intravesicular signals detected over time. These tri-block micelleplexes were designed to hijack the cells' natural receptor mediated endocytosis mechanism in order to escape the endosome and deliver the siRNA payload. Receptor mediated internalization can only be utilized by the folate decorated particles. It has been previously demonstrated that the uptake profiles of receptor mediated endocytosis is slower than adsorptive endocytosis and that the targeting benefit of these polyplexes is more strongly observed at later time points.(22) Additionally, it has been shown that FRα endocytosis of folic acid and FRα targeted nanoparticles utilize caveolae mediated endocytosis within lipid rafts, whereas non-targeted particles are likely to enter the cell via clathrin coated pits through adsorptive endocytosis.(48) Due to the nature of the different uptake mechanisms, the difference in intravesicular signal could be attributed to the uptake kinetics of the particles. Non-targeted particles may enter the cell at a faster rate than FRα mechanisms but may not be able to escape the endosome as efficiently as their targeted counterparts. This was noted in Figure 4 A where the targeted particles demonstrated a more efficient knockdown profile. These differences in kinetic and uptake mechanistic profiles can help explain the difference between their compartment signals shown in Figure 5 and the differences in luciferase knockdown efficacy over time (supplementary figure 2).

To measure size and morphology of the conjugates, we imaged randomly dispersed micellplexes which were air-dried on a glass coverslip. A uniform particle polydispersity with an average particle size of 152± 22 nm was observed, as seen in Figure 6. These sizes are consistent with the particle sizes of micelleplexes determined in previously published work using a Zetasizer Nano ZS.(22) These sizes, albeit slightly smaller than in Figure 2 A, are in agreement with the sizes of micelleplexes created in 5% glucose instead of a PBS solution, emphasizing the role of counter ions diffusing with the particles in a higher ionic strength dispersant which increase their hydrodynamic diameters.

In order to assess and compare binding probability of FRα with folic and folate decorated micelleplexes, we performed AFM force measurements. The AFM cantilever was first functionalized with an active FRα and experiments were run with varying substrates on a glass cover slip. Control experiments were performed with folate receptors on the cantilever

tip and a clean non-functionalized silicon substrate. In this case, there was little to no specific adhesion to the receptor; the binding probability for a blank substrate was 0.009. Next, over 1000 force measurements were recorded for each substrate with the FRα modified cantilever. In each case, the binding probability was determined by the number of force curves that show at least one rupture event divided by the total number of force measurements performed on the substrate. The binding probability for folic acid modified substrates to the folate receptors attached to the cantilever was 0.462. Conversely, the binding probability for the folate decorated micelleplexes to the active folate receptors attached to the cantilever was 0.573. The rupture force distributions on both folic acid and folate decorated micelleplexes at a 2 μm/s retract speed were also recorded. Rupture force histograms for folic acid and folate decorated micelleplexes are shown in Figure 7 A and B, respectively. For folate decorated micelleplexes, we found a most probable rupture force of 215.8 pN. This binding force was significantly ($p<10^{-22}$) higher compared to the most probable rupture force of 78.6 pN, which was observed for free folic acid only. This large difference is most likely due to multiple bonds formed on the folate decorated micelleplexes, leading to a higher binding probability and binding avidity of the multivalent folate decorated micelleplexes versus the affinity of folic acid to FRα. It should be noted that the same type of cantilever was functionalized under identical conditions for both experiments.

Multiple studies have tried to use a competitive inhibition setup to demonstrate that the addition of free folic acid to the system will outcompete the folate decorated nanoparticles for the binding to FRα. With this in mind, the kinetics of bond formation was observed between a FRα decorated cantilever and folate decorated micelleplexes. During the experiment, repetitive injections of free folic acid was added at fixed concentrations into the measurement cell. Figure 8 shows the binding probability of the decorated micelleplexes with FRα versus the injected folic acid concentration. Based on the cell uptake study shown in Figure 3, we hypothesized that low levels of free folic acid could only slightly decrease the binding probability of multivalent folate decorated micelleplexes having multiple binding sites on the cantilever. Therefore, we expected that they could not be displaced efficiently from the receptor by monovalent folic acid. Accordingly, it was observed that injection of free folic acid into the flow cell did not decrease the binding probability significantly until about 250-300 μM free FA. However, as the concentrations of free folic acid increased, a precipitous decrease of the binding probability was observed. These results are in full agreement with the uptake study in Figure 3 A-D. Earlier published work with free folic acid around 100 μM showed no significant inhibition of siRNA uptake between targeted and non-targeted micelleplexes, which can be explained by the results in Figure 8. At 250 μM, a slight inhibition of binding probability can be observed correlated with a significant decrease in siRNA uptake for the targeted micelleplexes, but unchanged uptake in the non-targeted formulation. At this concentration, a “sweet spot” seemed to have been reached where the free folic acid inhibited the folate receptor dependent endocytosis while not decreasing micelleplex stability. Even if increased average hydrodynamic diameters of the particles were observed at this concentration of free folic acid, apparently not all particles had aggregated and a large amount of particles was still in the size range for efficient endocytosis. As demonstrated at higher concentrations above 250 μM, the binding probability significantly drops off while in cell culture, the uptake of both targeted and non-

targeted formulations was significantly inhibited. Overall, the precipitous drop of binding probability above 250 μM of free folic acid can easily be explained by micelleplex instability in the presence of high concentrations of free folic acid. With the dissociation of the micelleplexes, the valency is decreased from multivalent complexes to monovalent conjugates which can be displaced from the receptor by the presence of excess monovalent ligand.

Limits of this AFM-based approach failed to consider, or to verify, the clustering of FRα. On the apical surface of the cell, FRα tend to cluster together on lipid rafts which is not obtainable through this approach. In a normal biological state, if the FRα cluster together, the multivalency of folate decorated micelleplexes can utilize the proximity of other FRα to create a tighter binding when compared to a free standing FRα. Unfortunately, with functionalizing the cantilever with FRα, receptor clustering can only be aimed for by adjusting the receptor concentration used for the functionalization.(49, 50) Lastly, in *in vitro* and *in vivo* experiments with FRα expressing cells, the addition of free folic acid can have several pharmacological effects on the cells which could inhibit binding and uptake. However, with this approach, we can only address any biophysical effects of receptor binding that happen.

## Summary and Conclusion

Targeted therapy has been on the forefront of developing new treatment options in the clinic. The ability to selectively target cancer cells while avoiding toxicity to healthy tissues has become the model outcome of drug delivery. Since the development of the field of nanomedicine in the late 2000's, the ability to easily modulate and alter delivery systems to fit the needs of one disease profile is achievable. It has been shown that multiple cell surface receptors are significantly over-expressed within a variety of disease states such as cancer and or inflammatory diseases. However, to target these receptors, specifically FRα, we believe there needs to be more optimization in the models in order to confidently claim that receptor targeting is being utilized when the ligand is added to the nanoparticle. Multiple experiments other than the excess addition of the targeting ligand, as discussed in this paper, can further elucidate the multivalent targeting advantage gained when a targeting ligand (e.g. folic acid) is added to a drug delivery system. Here, FRα binding properties of micelleplexes made with folate targeted triblock copolymers were evaluated. The sizes and zeta potentials of the micelleplexes were verified with DLS and AFM in a PBS solution and compared with previously published results.(22) The sizes for both techniques were within the 200-250 nm threshold with a slightly positive zeta potential. The hydrodynamic diameters were slightly larger than previously reported due to the change in solvents from 5% to PBS. AFM data with a modified cantilever demonstrated that the multivalent micelleplexes bind at a higher probability and a with a stronger force than free folic acid. Receptor mediated endocytosis and knockdown kinetics were studied with the monensin assay and luciferase assay. As shown, the targeted micelleplexes resulted in a greater accumulation in the cytosol over time which leads to a significant targeting advantage to luciferase knockdown after 48 hours when compared to the non-targeted micelleplex. Additionally, due to the slow recycling of the FRα over time as well as the propensity of the receptor to recycle back to the surface with its cargo, a greater amount of the micelleplexes were found extracellularly and

intravesicularly over time. Collectively, these data suggest that a simple design of adding excess folic acid ligand to an uptake study may not prove or disprove receptor-mediated endocytosis. Further studies, as described here, should be carried out to investigate a targeting advantage that is gained through ligand conjugation. In this manuscript, the targeted micelleplexes have a higher degree of binding and stronger binding than folic acid. This results in an inherent targeting advantage that cannot be overcome by adding excess ligand into the solution without jeopardizing the entire system.

## Supplementary Material

Refer to Web version on PubMed Central for supplementary material.

## Acknowledgments

**Funding Sources**: This work was supported by the Excellence Cluster Nanosystems Initiative Munich (NIM), the Wayne State Start-Up and NanoIncubator grant to Olivia Merkel as well as the Ruth L. Kirschstein National Research Award T32-CA009531 fellowship and Predoctoral Fellowship in Cancer Research from the DeRoy Testamentary Foundation to Steven Jones. The NIH Center grant P30CA22453 supporting the Wayne State Microscopy, Imaging and Cytometry Resources (MICR), is gratefully acknowledged. Christoph Hohmann (NIM) is sincerely acknowledged for preparing the table of contents graphic art.

## References

1. Xu S, Olenyuk BZ, Okamoto CT, Hamm-Alvarez SF. Targeting receptor-mediated endocytotic pathways with nanoparticles: rationale and advances. Adv Drug Deliv Rev. 2013; 65(1):121–38. [PubMed: 23026636]
2. Bazak R, Houri M, Achy SE, Kamel S, Refaat T. Cancer active targeting by nanoparticles: a comprehensive review of literature. Journal of cancer research and clinical oncology. 2015; 141(5): 769–84. [PubMed: 25005786]
3. Assaraf YG, Leamon CP, Reddy JA. The folate receptor as a rational therapeutic target for personalized cancer treatment. Drug resistance updates : reviews and commentaries in antimicrobial and anticancer chemotherapy. 2014; 17(4-6):89–95. [PubMed: 25457975]
4. Lu Y, Low PS. Folate-mediated delivery of macromolecular anticancer therapeutic agents. Adv Drug Deliv Rev. 2002; 54(5):675–93. [PubMed: 12204598]
5. Hilgenbrink AR, Low PS. Folate receptor-mediated drug targeting: from therapeutics to diagnostics. Journal of pharmaceutical sciences. 2005; 94(10):2135–46. [PubMed: 16136558]
6. Bandara NA, Hansen MJ, Low PS. Effect of receptor occupancy on folate receptor internalization. Mol Pharm. 2014; 11(3):1007–13. [PubMed: 24446917]
7. Leamon CP, Low PS. Delivery of macromolecules into living cells: a method that exploits folate receptor endocytosis. Proc Natl Acad Sci U S A. 1991; 88(13):5572–6. [PubMed: 2062838]
8. Vergote I, Leamon CP. Vintafolide: a novel targeted therapy for the treatment of folate receptor expressing tumors. Therapeutic advances in medical oncology. 2015; 7(4):206–18. [PubMed: 26136852]
9. Lorusso PM, Edelman MJ, Bever SL, Forman KM, Pilat M, Quinn MF, et al. Phase I study of folate conjugate EC145 (Vintafolide) in patients with refractory solid tumors. Journal of clinical oncology : official journal of the American Society of Clinical Oncology. 2012; 30(32):4011–6. [PubMed: 23032618]
10. Reddy JA, Dorton R, Bloomfield A, Nelson M, Vetzel M, Guan J, et al. Rational combination therapy of vintafolide (EC145) with commonly used chemotherapeutic drugs. Clinical cancer research : an official journal of the American Association for Cancer Research. 2014; 20(8):2104–14. [PubMed: 24429878]

11. Dhawan D, Ramos-Vara JA, Naughton JF, Cheng L, Low PS, Rothenbuhler R, et al. Targeting folate receptors to treat invasive urinary bladder cancer. Cancer Res. 2013; 73(2):875–84. [PubMed: 23204225]
12. Silpe JE, Sumit M, Thomas TP, Huang B, Kotlyar A, van Dongen MA, et al. Avidity Modulation of Folate-Targeted Multivalent Dendrimers for Evaluating Biophysical Models of Cancer Targeting Nanoparticles. ACS chemical biology. 2013; 8(9):2063–71. [PubMed: 23855478]
13. Stella B, Arpicco S, Peracchia MT, Desmaele D, Hoebeke J, Renoir M, et al. Design of folic acid-conjugated nanoparticles for drug targeting. Journal of pharmaceutical sciences. 2000; 89(11): 1452–64. [PubMed: 11015690]
14. Hong S, Leroueil PR, Majoros IJ, Orr BG, Baker JR Jr, Banaszak Holl MM. The binding avidity of a nanoparticle-based multivalent targeted drug delivery platform. Chemistry & biology. 2007; 14(1):107–15. [PubMed: 17254956]
15. Kamen BA, Smith AK. A review of folate receptor alpha cycling and 5-methyltetrahydrofolate accumulation with an emphasis on cell models in vitro. Adv Drug Deliv Rev. 2004; 56(8):1085–97. [PubMed: 15094208]
16. Movahedi K, Schoonooghe S, Laoui D, Houbracken I, Waelput W, Breckpot K, et al. Nanobody-based targeting of the macrophage mannose receptor for effective in vivo imaging of tumor-associated macrophages. Cancer Res. 2012; 72(16):4165–77. [PubMed: 22719068]
17. Endres T, Zheng M, Kilic A, Turowska A, Beck-Broichsitter M, Renz H, et al. Amphiphilic biodegradable PEG-PCL-PEI triblock copolymers for FRET-capable in vitro and in vivo delivery of siRNA and quantum dots. Mol Pharm. 2014; 11(4):1273–81. [PubMed: 24592902]
18. Zheng M, Librizzi D, Kilic A, Liu Y, Renz H, Merkel OM, et al. Enhancing in vivo circulation and siRNA delivery with biodegradable polyethylenimine-graft-polycaprolactone-block-poly(ethylene glycol) copolymers. Biomaterials. 2012; 33(27):6551–8. [PubMed: 22710127]
19. Liu Y, Samsonova O, Sproat B, Merkel O, Kissel T. Biophysical characterization of hyper-branched polyethylenimine-graft-polycaprolactone-block-mono-methoxyl-poly(ethylene glycol) copolymers (hy-PEI-PCL-mPEG) for siRNA delivery. J Control Release. 2011; 153(3):262–8. [PubMed: 21549166]
20. Zheng M, Liu Y, Samsonova O, Endres T, Merkel O, Kissel T. Amphiphilic and biodegradable hy-PEI-g-PCL-b-PEG copolymers efficiently mediate transgene expression depending on their graft density. International journal of pharmaceutics. 2012; 427(1):80–7. [PubMed: 21600970]
21. Liu L, Zheng M, Librizzi D, Renette T, Merkel OM, Kissel T. Efficient and Tumor Targeted siRNA Delivery by Polyethylenimine-graft-polycaprolactone-block-poly(ethylene glycol)-folate (PEI-PCL-PEG-Fol). Mol Pharm. 2016; 13(1):134–43. [PubMed: 26641134]
22. Jones SK, Lizzio V, Merkel OM. Folate Receptor Targeted Delivery of siRNA and Paclitaxel to Ovarian Cancer Cells via Folate Conjugated Triblock Copolymer to Overcome TLR4 Driven Chemotherapy Resistance. Biomacromolecules. 2016; 17(1):76–87. [PubMed: 26636884]
23. Merkel OM, Beyerle A, Beckmann BM, Zheng M, Hartmann RK, Stoger T, et al. Polymer-related off-target effects in non-viral siRNA delivery. Biomaterials. 2011; 32(9):2388–98. [PubMed: 21183213]
24. Merkel OM, Beyerle A, Beckmann BM, Zheng M, Hartmann RK, Stöger T, et al. Polymer-related off-target effects in non-viral siRNA delivery. Biomaterials. 2011; 32(9):2388–98. [PubMed: 21183213]
25. Corona G, Giannini F, Fabris M, Toffoli G, Boiocchi M. Role of folate receptor and reduced folate carrier in the transport of 5-methyltetrahydrofolic acid in human ovarian carcinoma cells. International journal of cancer. 1998; 75(1):125–33. [PubMed: 9426700]
26. Campbell IG, Jones TA, Foulkes WD, Trowsdale J. Folate-binding protein is a marker for ovarian cancer. Cancer Res. 1991; 51(19):5329–38. [PubMed: 1717147]
27. He C, Hu Y, Yin L, Tang C, Yin C. Effects of particle size and surface charge on cellular uptake and biodistribution of polymeric nanoparticles. Biomaterials. 2010; 31(13):3657–66. [PubMed: 20138662]
28. Storm G, Belliot SO, Daemen T, Lasic DD. Surface modification of nanoparticles to oppose uptake by the mononuclear phagocyte system. Advanced Drug Delivery Reviews. 1995; 17(1):31–48.

29. Jiang W, Kim BY, Rutka JT, Chan WC. Nanoparticle-mediated cellular response is size-dependent. Nature nanotechnology. 2008; 3(3):145–50.
30. Bhattacharya D, Das M, Mishra D, Banerjee I, Sahu SK, Maiti TK, et al. Folate receptor targeted, carboxymethyl chitosan functionalized iron oxide nanoparticles: a novel ultradispersed nanoconjugates for bimodal imaging. Nanoscale. 2011; 3(4):1653–62. [PubMed: 21331392]
31. Li TS, Yawata T, Honke K. Efficient siRNA delivery and tumor accumulation mediated by ionically cross-linked folic acid-poly(ethylene glycol)-chitosan oligosaccharide lactate nanoparticles: for the potential targeted ovarian cancer gene therapy. European journal of pharmaceutical sciences : official journal of the European Federation for Pharmaceutical Sciences. 2014; 52:48–61. [PubMed: 24178005]
32. Esmaeili F, Ghahremani MH, Ostad SN, Atyabi F, Seyedabadi M, Malekshahi MR, et al. Folate-receptor-targeted delivery of docetaxel nanoparticles prepared by PLGA-PEG-folate conjugate. Journal of drug targeting. 2008; 16(5):415–23. [PubMed: 18569286]
33. Krais A, Wortmann L, Hermanns L, Feliu N, Vahter M, Stucky S, et al. Targeted uptake of folic acid-functionalized iron oxide nanoparticles by ovarian cancer cells in the presence but not in the absence of serum. Nanomedicine : nanotechnology, biology, and medicine. 2014; 10(7):1421–31.
34. Su C, Li H, Shi Y, Wang G, Liu L, Zhao L, et al. Carboxymethyl-beta-cyclodextrin conjugated nanoparticles facilitate therapy for folate receptor-positive tumor with the mediation of folic acid. International journal of pharmaceutics. 2014; 474(1-2):202–11. [PubMed: 25149123]
35. Benoit DS, Srinivasan S, Shubin AD, Stayton PS. Synthesis of folate-functionalized RAFT polymers for targeted siRNA delivery. Biomacromolecules. 2011; 12(7):2708–14. [PubMed: 21634800]
36. Arima H, Yoshimatsu A, Ikeda H, Ohyama A, Motoyama K, Higashi T, et al. Folate-PEG-appended dendrimer conjugate with alpha-cyclodextrin as a novel cancer cell-selective siRNA delivery carrier. Mol Pharm. 2012; 9(9):2591–604. [PubMed: 22873579]
37. Fernandes JC, Qiu X, Winnik FM, Benderdour M, Zhang X, Dai K, et al. Low molecular weight chitosan conjugated with folate for siRNA delivery in vitro: optimization studies. Int J Nanomedicine. 2012; 7:5833–45. [PubMed: 23209368]
38. Elias DR, Poloukhtine A, Popik V, Tsourkas A. Effect of ligand density, receptor density, and nanoparticle size on cell targeting. Nanomedicine : nanotechnology, biology, and medicine. 2013; 9(2):194–201.
39. Cruz LJ, Tacken PJ, Pots JM, Torensma R, Buschow SI, Figdor CG. Comparison of antibodies and carbohydrates to target vaccines to human dendritic cells via DC-SIGN. Biomaterials. 2012; 33(16):4229–39. [PubMed: 22410170]
40. Paulos CM, Reddy JA, Leamon CP, Turk MJ, Low PS. Ligand binding and kinetics of folate receptor recycling in vivo: impact on receptor-mediated drug delivery. Molecular pharmacology. 2004; 66(6):1406–14. [PubMed: 15371560]
41. Lee RJ, Low PS. Delivery of liposomes into cultured KB cells via folate receptor-mediated endocytosis. J Biol Chem. 1994; 269(5):3198–204. [PubMed: 8106354]
42. Reddy JA, Abburi C, Hofland H, Howard SJ, Vlahov I, Wils P, et al. Folate-targeted, cationic liposome-mediated gene transfer into disseminated peritoneal tumors. Gene Ther. 2002; 9(22): 1542–50. [PubMed: 12407426]
43. Ciuchi F, Di Nicola G, Franz H, Gottarelli G, Mariani P, Ponzi Bossi MG, et al. Self-Recognition and Self-Assembly of Folic Acid Salts: Columnar Liquid Crystalline Polymorphism and the Column Growth Process. Journal of the American Chemical Society. 1994; 116(16):7064–71.
44. Moody PR, Sayers EJ, Magnusson JP, Alexander C, Borri P, Watson P, et al. Receptor Crosslinking: A General Method to Trigger Internalization and Lysosomal Targeting of Therapeutic Receptor:Ligand Complexes. Molecular Therapy. 2015; 23(12):1888–98. [PubMed: 26412588]
45. Mislick KA, Baldeschwieler JD, Kayyem JF, Meade TJ. Transfection of folate-polylysine DNA complexes: evidence for lysosomal delivery. Bioconjugate chemistry. 1995; 6(5):512–5. [PubMed: 8974447]
46. Phillips MI. Antisense Technology; Part A: General Methods, Methods and Delivery, and RNA Studies. Methods in Enzymology. 2000; 313

47. Wileman T, Boshans RL, Schlesinger P, Stahl P. Monensin inhibits recycling of macrophage mannose-glycoprotein receptors and ligand delivery to lysosomes. Biochem J. 1984; 220(3):665–75. [PubMed: 6087792]

48. Matsue H, Rothberg KG, Takashima A, Kamen BA, Anderson RG, Lacey SW. Folate receptor allows cells to grow in low concentrations of 5-methyltetrahydrofolate. Proceedings of the National Academy of Sciences. 1992; 89(13):6006–9.

49. Smart EJ, Mineo C, Anderson RG. Clustered folate receptors deliver 5-methyltetrahydrofolate to cytoplasm of MA104 cells. The Journal of cell biology. 1996; 134(5):1169–77. [PubMed: 8794859]

50. Wu M, Fan J, Gunning W, Ratnam M. Clustering of GPI-anchored folate receptor independent of both cross-linking and association with caveolin. The Journal of membrane biology. 1997; 159(2): 137–47. [PubMed: 9307440]

51. Xie Y, Kim NH, Nadithe V, Schalk D, Thakur A, Kilic A, et al. Targeted delivery of siRNA to activated T cells via transferrin-polyethylenimine (Tf-PEI) as a potential therapy of asthma. J Control Release. 2016; 229:120–9. [PubMed: 27001893]

52. Sadat SM, Saeidnia S, Nazarali AJ, Haddadi A. Nano-pharmaceutical formulations for targeted drug delivery against HER2 in breast cancer. Current cancer drug targets. 2015; 15(1):71–86. [PubMed: 25564255]

53. Ragelle H, Colombo S, Pourcelle V, Vanvarenberg K, Vandermeulen G, Bouzin C, et al. Intracellular siRNA delivery dynamics of integrin-targeted, PEGylated chitosan-poly(ethylene imine) hybrid nanoparticles: A mechanistic insight. J Control Release. 2015; 211:1–9. [PubMed: 25989603]

## Abbreviations

| | |
|---|---|
| **siRNA** | small interfering RNA |
| **FRα** | folate receptor alpha |
| **AFM** | Atomic Force Microscopy |


**Figure 1.**

Folate Receptor Alpha (FRα) Expression for Ovarian Cancer Cell Lines: Two ovarian cancer cell lines which are known to over-express FRα were tested for their FRα expression levels via flow cytometry compared to a lung cancer cell line which is known to express only basal levels of FRα. Each sample was stained with a primary FRα specific antibody followed by a fluorescent secondary antibody, *$p<0.05$.

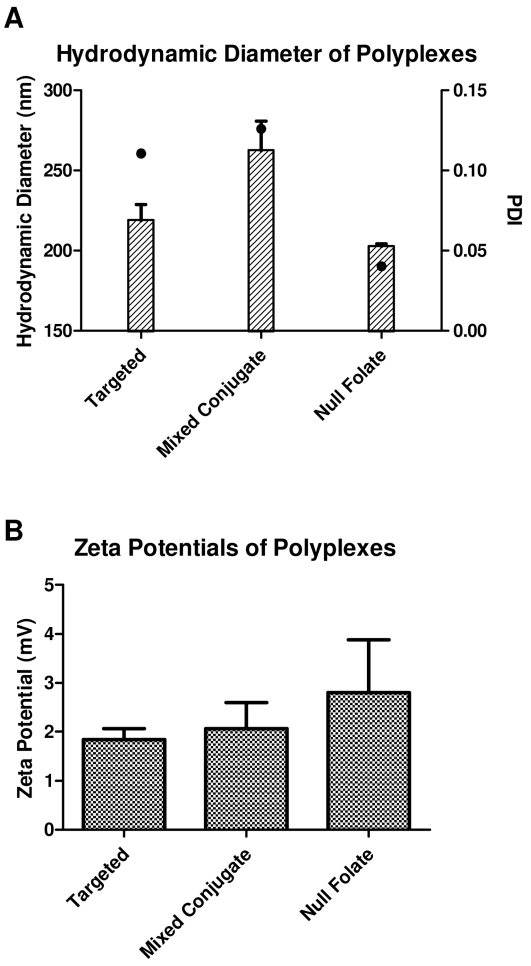


**Figure 2.**

Hydrodynamic diameter and Zeta Potential Measurements: Micelleplexes made of three different triblock co-polymers were analyzed by DLS and LDA at N/P ratio 5 in PBS. Two folate decorated co-polymers (targeted and mixed conjugate) as well as a null folate co-polymer were analyzed. Hydrodynamic diameters (bars) and PDI (dots) are presented in Figure 2 A, and zeta potentials are measured in Figure 2 B.

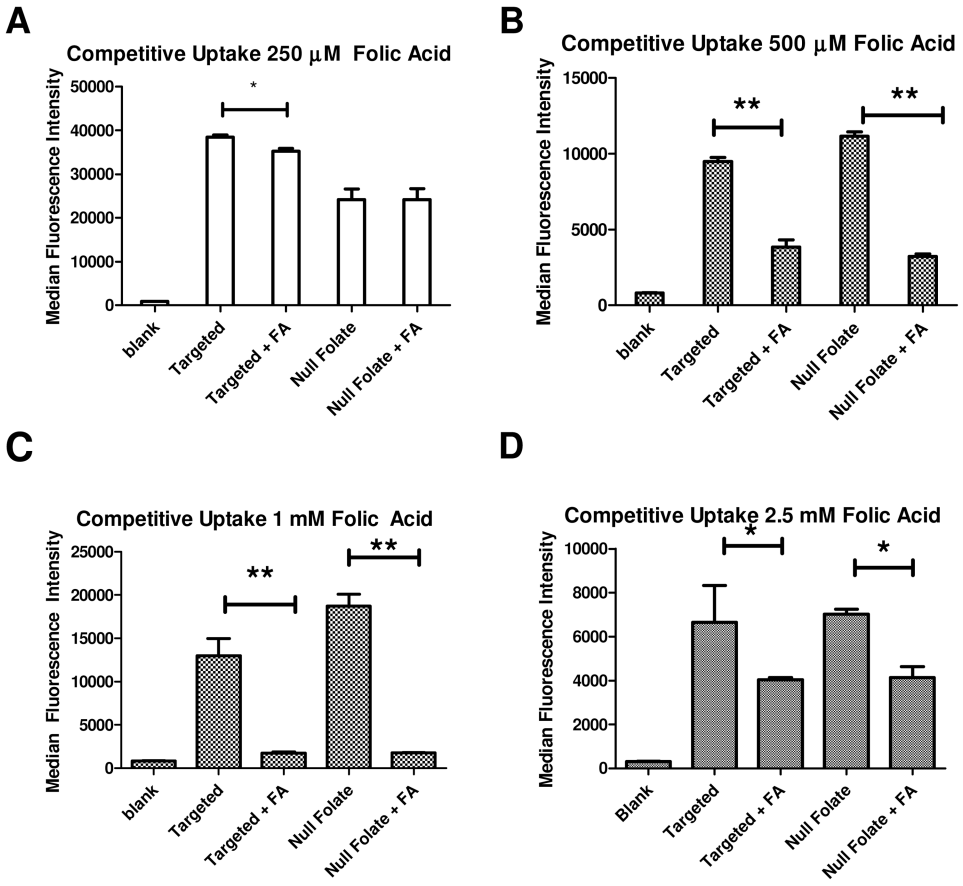


**Figure 3.**

Micelleplex Competitive Uptake Studies Using Flow Cytometry (A-D): Uptake Studies in SKOV-3 cells compared for targeted and null folate micelleplexes at varying concentrations of free folic acid. *p<0.05, **p<0.01.

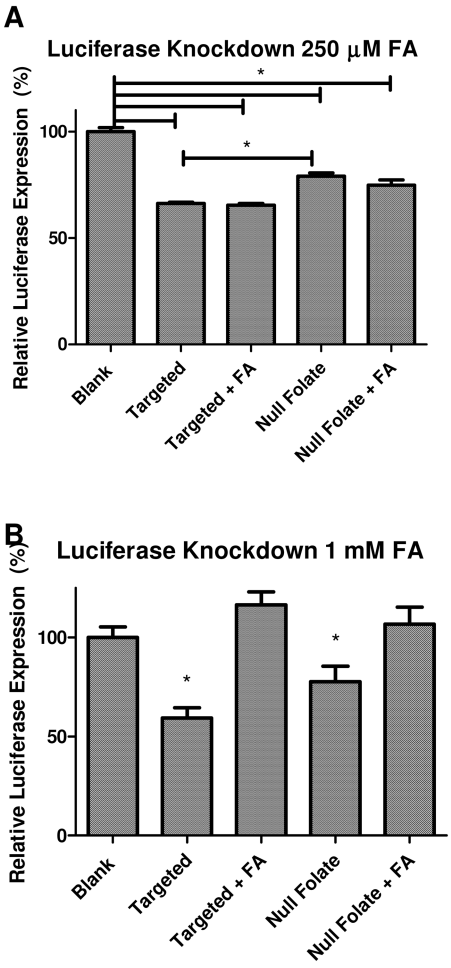


**Figure 4.**

Luciferase Assay Competitive Knockdown: Luciferase assay in SKOV-3/LUC cells assessing firefly luciferase knockdown 48 h post transfection at 250 μM (A), and 1 mM (B) of free folic acid. * $p < 0.05$

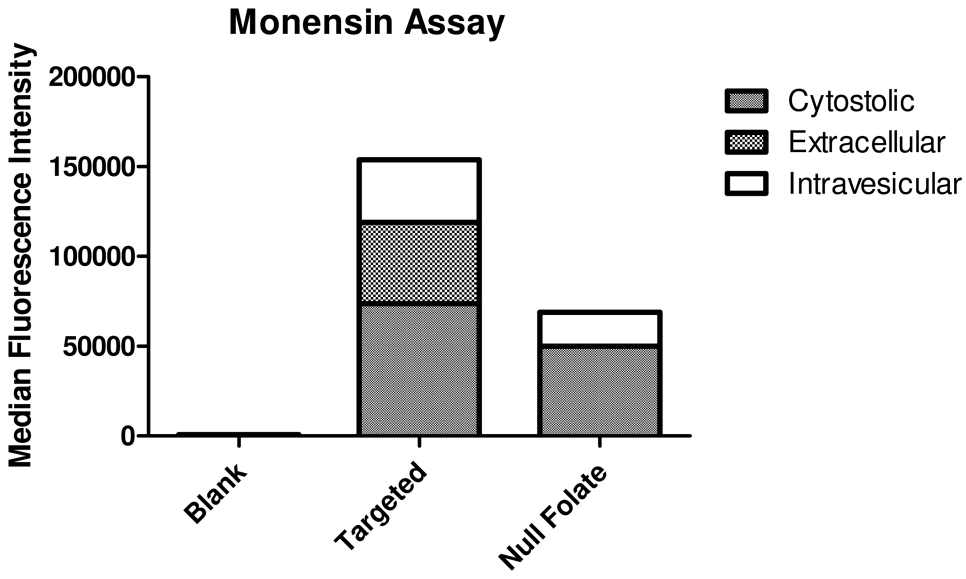


**Figure 5.**

Monensin uptake assay: Uptake study with trypan blue and monensin treatment to assess localization of siRNA within SKOV-3 cells 48 h after transfection.

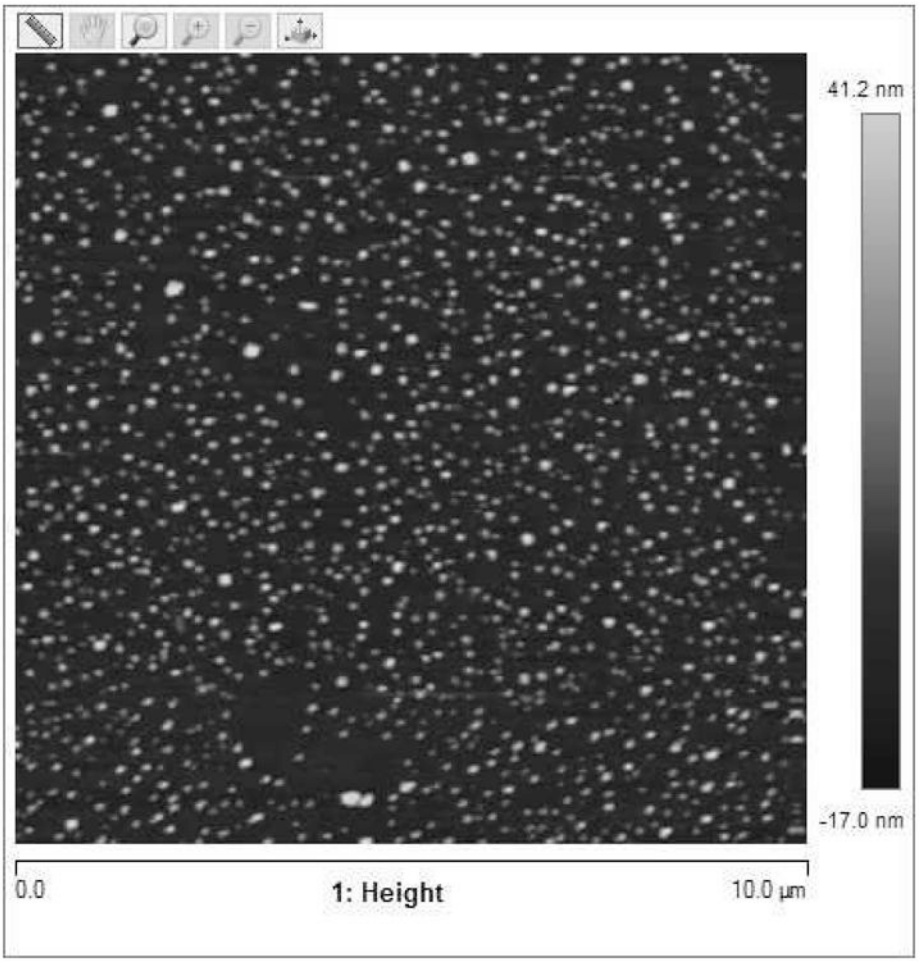


**Figure 6.**

AFM images of micelleplexes: Topographical image of micelleplexes on a 25*25mm glass coverslip with scan size of 10 μm.

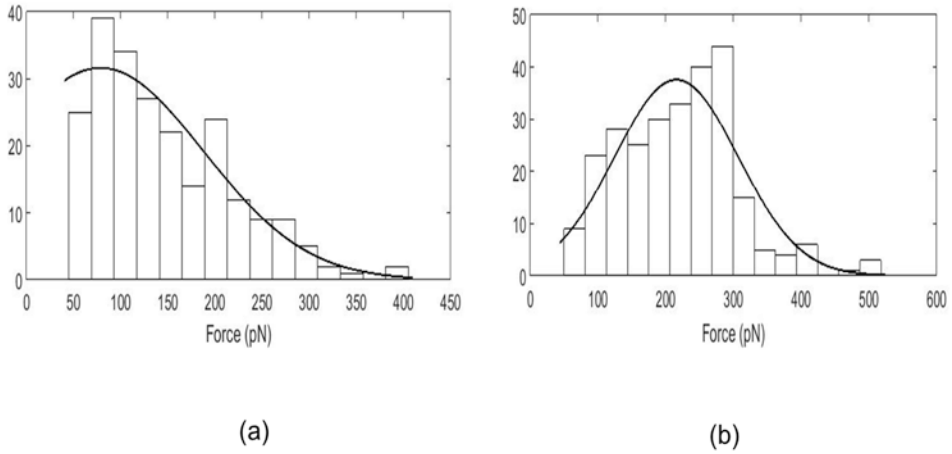


**Figure 7.**

(a) Rupture force histogram plotted for substrate functionalized with free folic acid, (b) Rupture force histogram for substrate functionalized with folate decorated nanoparticles.

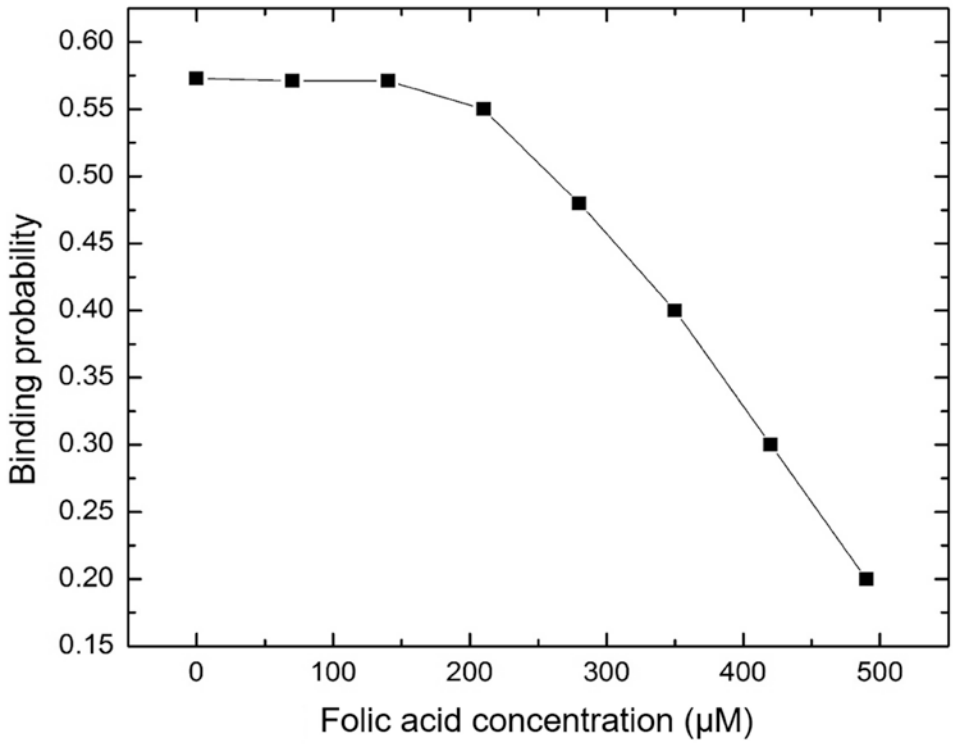


**Figure 8.**

Binding probability versus concentration of folic acid after injecting folic acid in the flow cell of a substrate functionalized with folate decorated nanoparticles with a folate receptor functionalized cantilever tip.